



Microstructure and mechanical properties of Sn–1.0Ag–0.5Cu solder with minor Zn additions

Y. M. Leong¹ · A. S. M. A. Haseeb¹ · Hiroshi Nishikawa² · Omid Mokhtari²

Received: 15 March 2019 / Accepted: 18 May 2019 / Published online: 31 May 2019
© Springer Science+Business Media, LLC, part of Springer Nature 2019

Abstract

Low silver (Ag) solder alloys e.g., SAC 105 (Sn–1.0Ag–0.5Cu) have attracted a great deal of attention recently due to economic concerns and improved in impact resistance as compared to other SAC solder with higher silver content. This work studies the influence of addition of minor zinc (0.1–0.5 wt%) to SAC105 on the interfacial structure between solder and copper substrate during reflow and after aging. Zn has shown significant solubility in Cu–Sn intermetallic compound (IMC) and formed $\text{Cu}_6(\text{Sn,Zn})_5$ which resided in the bulk microstructure and at the solder/Cu interface. Results reveal that minor Zn addition decreased the thickness of interfacial Cu_6Sn_5 IMC after reflow and significantly suppressed the growth of interfacial Cu_3Sn after thermal aging without changing the IMC's morphology. It is suggested that Zn exerts its influence by stabilizing $\text{Cu}_6(\text{Sn,Zn})_5$ and hindering the flow of Sn and Cu atoms at the solder/IMC and IMC/Cu interface. Nanoindentation results showed that $\text{Cu}_6(\text{Sn,Zn})_5$ exhibited a higher hardness in comparison to Cu_6Sn_5 and creep performance of SAC + Zn has improved in comparison to that of SAC105.

1 Introduction

It has been more than a decade since the restriction of lead usage in the electronics industry [1]. Sn based solder, especially Sn–Ag–Cu solder have been one of the favourable replacements for Sn–Pb solders. Yet, it still has some drawbacks when compared to its lead containing counterpart. Some of these drawbacks include: (i) higher melting temperature of SAC solder (T_m of eutectic Sn–3.8Ag–0.7Cu = 217 °C, T_m of eutectic SnPb = 183 °C), which may damage the printed circuit board (PCB) and other electronic components; (ii) inferior wetting as compared to SnPb solder; and (iii) relatively high undercooling (10–30 °C), which promotes brittle plate-like Ag_3Sn formation leading to reliability issues [2, 3]. In recent years, there seems to be a growing trend on research on low Ag

solder, e.g. SAC105, or no Ag solder in order to reduce the cost of SAC solder and to hinder the formation of Ag_3Sn . SAC105 was reported to perform better in drop impact tests as compared to eutectic SAC, which is very important in the reliability of microelectronics [4]. However, it had a few drawbacks, such as higher liquidus temperature ($T_{\text{SAC105}} = 225$ °C; $T_{\text{SAC387}} = 219$ °C), which would require a higher reflow profile and it also reported to have lower thermal cyclic performance [4, 5]. These pros and cons of SAC 105 have prompted researchers to add in minor amount of fourth alloying element to improve its drawbacks.

Fourth minor alloying elements that have been investigated include Ni, Fe, Sb, In, Co, Ce, Pd, Mn, Al, Zn, Ti and In [6–9]. Many have studied their effects on the microstructure (bulk microstructure and interfacial IMC growth) and mechanical properties. Improvement in microstructure such as refinement of the bulk microstructure and suppressing or a change in the morphology of Cu–Sn IMC have been reported [10], Laurila et al. had categorized those minor alloying elements that have effects on the Cu–Sn IMC growth into two categories. The first category consists of elements that was soluble in Cu–Sn IMCs, while the second category consists of those elements that has no solubility in Cu–Sn IMCs [10]. For element in category 1, thermodynamic argument was used to explain the effect on the IMC growth, where they stabilize Cu_6Sn_5 and further

✉ A. S. M. A. Haseeb
haseeb@um.edu.my

Y. M. Leong
leongyeemei@siswa.um.edu.my

¹ Centre for Advanced Materials, Department of Mechanical Engineering, Faculty of Engineering, University of Malaya, 50603 Kuala Lumpur, Malaysia

² Joining and Welding Research Institute, Osaka University, Osaka 567-0047, Japan

lead to the suppression of the Cu_3Sn growth. On the other hand, since the elements in category 2 do not dissolve in IMC, therefore they could impart their influence on the growth of IMC layers indirectly by affecting the activity of Sn or Cu [10]. Besides that, studies have shown improvements in mechanical properties by adding fourth alloying element such as tensile strength [6], hardness [11], shear strength [9], creep resistance [5], and impact resistance [6]. Addition of minor alloying element into solder modified the microstructure of solder joints and thus improved its mechanical properties. Microstructures of a solder could be altered by (i) microstructure refinement of the solder matrix; (ii) brittle IMC growth suppression at the solder matrix or Sn/Cu interface; and (iii) changing the IMC's morphology at the solder matrix or Sn/Cu interface [10].

Out of the fourth alloying elements studied so far, the addition Zn was among those that have attracted much attentions. Many studies have reported the addition of Zn, both as nanoparticles and as minor alloying element [12–16]. Studies on Zn as minor alloying element have been done to investigate its effect on thermal properties, microstructures and mechanical properties [14–16]. Zn was found to lower the undercooling of SAC solder significantly [16]. Besides, many researches have reported that very small amount Zn was found to hinder the growth of Cu_3Sn during solid state annealing, even at an addition of a low amount such as 0.2 wt% [10, 16]. Zn is soluble in the IMC layers (in this case both Cu_6Sn_5 and Cu_3Sn). Reported solubility values of Zn are 6 at.% in Cu_6Sn_5 and 9 at.% in Cu_3Sn [17]. Yu et al. reported that solubility of Zn as low as 0.8–0.21 at.% in Cu_6Sn_5 promotes phase stabilization of hexagonal $\eta\text{-Cu}_6\text{Sn}_5$ from transforming into monoclinic $\eta'\text{-Cu}_6\text{Sn}_5$ even after high temperature aging [18]. The stabilization of hexagonal $\eta\text{-Cu}_6\text{Sn}_5$ could prevent the volume change of Cu_6Sn_5 , and thereby improving the reliability of the solder joints. Besides, Chen et al. reported that incorporation of Zn in Cu_6Sn_5 can increase the Young's modulus and hardness of $\eta\text{-Cu}_6\text{Sn}_5$ compound [19].

Cho et al. has reported that the reduction of Cu_3Sn IMC growth by addition of Zn was beneficial in suppressing Kirkendall voids at the IMC/Cu interface upon thermal aging [14]. The suppressions of IMC and the reduction of voids at the interface have been reported to improve the drop impact and shear strength of the solder [14]. Hence, the addition of Zn seems promising in improving the quality of solder joint. However, there have been some pullbacks and concerns for using Zn as Zn is highly susceptible to oxidation and can cause degradation of wettability. Besides that, when addition of Zn was more than 0.8 wt%, formation of Cu_5Zn_8 layer was found at the solder/Cu interface, Cu_5Zn_8 was reported to be detrimental to the reliability of solder joint [13]. Thus, the amount of Zn added in solder should be carefully controlled,

as it has been reported that <0.4 wt% of Zn in solder effective without degrading other properties [12].

Information of mechanical properties of solder joint is fundamental to the design of reliable microelectronic devices. Nowadays, solder joints can have dimension as small as few micro-meters. Hence mechanical characterization based on conventional tensile or creep test obtained from bulk single rods may not always be appropriate to represent the mechanical properties of the solder joints [20, 21]. Thus, nanoindentation has been explored and has become an important modern mechanical testing equipment. Due to its ability to measure accurately in nanoscales, it has become a powerful tools in characterizing of the Young's modulus, hardness and creep behaviour of the various microphases in solder joints [22, 23]. Information on improving the mechanical properties of Cu_6Sn_5 is especially important in the mechanical reliability of new lead-free solder interconnects as Cu_6Sn_5 is a commonly formed IMC between Sn based solder and Cu substrate. A few studies have reported that Co, Mn, and Ni (from category 1) which was soluble in Cu–Sn IMC has changed the nanomechanical properties of Cu_6Sn_5 and Cu_3Sn [24–28]. As mentioned earlier on, Zn was soluble in Cu_6Sn_5 and Cu_3Sn , thus understanding the nanomechanical properties of $\text{Cu}_6(\text{Zn}, \text{Sn})_5$ is vital in order to understand the deformation behaviour and failure mechanisms of solder joints. Besides that, studies on nanomechanical properties of the relatively soft bulk solder which constitute the major of solder composition is also important. Till date, Chen et al. had studied the nanomechanical properties of $\text{Cu}_6\text{Zn}_{0.5}\text{Sn}_{4.5}$, where their results show that Zn addition can increase the Young's modulus and hardness of the $\eta\text{-Cu}_6\text{Zn}_{0.5}\text{Sn}_{4.5}$ compound [19].

In summary, many studies have been done on the effect of Zn on the SAC solder, although the Cu_3Sn IMC suppression appear to be consistent on all studies, there is a lack of knowledge regarding the Zn distribution in $\text{Cu}_6(\text{Zn}, \text{Sn})_5$ and their relationship with the nanomechanical properties of $\text{Cu}_6(\text{Zn}, \text{Sn})_5$. This work studies the effect of Zn (0.1–0.5 wt%) on microstructure and nanomechanical properties on the bulk and interfacial IMC between SAC105 and Cu substrate. Zn was added at a lower percentage of 0.1–0.5 wt%, as higher percentage of Zn may form Cu_5Zn_8 and other Zn intermetallic compound. This work concentrates on the distribution of Zn in $\text{Cu}_6(\text{Zn}, \text{Sn})_5$ and its relationship with the nanomechanical properties of $\text{Cu}_6(\text{Zn}, \text{Sn})_5$ during reflow and isothermal aging. Effect of Zn on the nanomechanical properties such as hardness, Young's Modulus and creep behaviour of the bulk solder are investigated as well.

2 Methodology

SAC105 + xZn (where $x = 0, 0.1, 0.3, 0.5$ wt%) alloys used in this experiment were supplied by Beijing Compo Advanced Technology Co Ltd. Sn, Ag, Cu and Zn were melted in medium frequency induction furnace at 300 °C for 10 min and were stirred for every 3 min. Molten solder mixture was casted in rod shape with diameter of 0.7 cm and length of 15 cm. The rod-shaped solidified sample alloys were then cut into thin disk (diameter = 6.5 mm, thickness = 1 mm) by using wire-cut electric discharge machining (EDM).

As-cast solder sample was prepared for microstructure investigation by using grinding and polishing methods mentioned in previous studies [29]. Copper substrates (Bottom Cu substrates—15 mm × 15 mm × 3 mm; Top Cu substrates—7 mm diameter, 2 mm thickness) were prepared by following cleaning processes mentioned in previous studies prior to soldering [29]. Water soluble flux Sparkle Flux WF-6317 from Senju Metal Industry was spread uniformly on the surface of both top and bottom Cu substrates. SAC-xZn thin disc were then sandwiched in between the top and bottom copper substrate. Samples were then subjected to reflow, under a compression pressure of 5 MPa at 270 °C for 120 s. After reflow, samples were rinsed under running distilled water to remove the residual flux. The reflowed samples were then cross sectioned and prepared for microstructural investigation by using standard metallographic techniques. The microstructure of the solder joints and the composition of IMC were investigated by using FESEM and EDS. Zn distribution in IMC was investigated by Electron Probe Micro-Analyzer (EPMA). IMC thickness was calculated by dividing the IMC area by the length of IMC. The area and length of IMC were obtained from the FESEM micrographs by using image analysis. Average thickness values were reported from measurement obtained from five micrographs. In order to expose the interfacial IMC for top view observation, samples were etched in an etchant (93% CH₃OH, 5% HNO₃, 2% HCl) for ~ 18–20 h to remove the solder matrix.

In this study, Hysitron Ubi-750 nanoindenter machine was used to carried out all the nanoindentation testing. Two nanoindentation mode were carried out on the samples: Quasi-static and Continuous dynamic measurement. Quasi-static indentation was conducted on the bulk microstructure (maximum load = 0.1 N, holding time = 2 s, loading rate and unloading rate = 16.67 N/s). For each sample, indentation arrays of 100 indentations were applied across the region of interest and the mean values were obtained. Each indent was spaced approximately 10 μm apart so that the impression from one indentation does not influence the readings taken for the next indentation. Continuous

dynamic measurement test was performed on interfacial IMC (maximum load = 1000 μN, holding time = 2 s, loading rate and unloading rate = 16.67 μN/s). Hardness (H) and elastic modulus (E) were obtained by analysing load–displacement data using Oliver and Pharr's method [30]. In continuous dynamic measurement, H and complex modulus could be obtained as a function of indentation depth. Complex modulus (also called dynamic measurement) measures the stress to strain ratio under vibratory conditions [31]. Nanoindentation creep was performed on the bulk microstructure of the specimens, loading rate of 1 mN/s, maximum load 10 mN, holding time of 900 s. For each sample, 20 indentations were performed to get the average values.

3 Results

3.1 Microstructure

Figure 1 shows the cross-sectional micrographs of the bulk microstructure of as-received solders and reflowed solders. From the micrograph, as-received SAC105 samples show primary Sn phase (lighter contrast) and EDX results indicate that the darker contrast phase is Cu₆Sn₅. In the as received SAC105, Cu₆Sn₅ formed a continuous network and fine Ag₃Sn particles are also seen at some places under high magnification. With the addition of Zn, a finer Cu₆Sn₅ phase network are seen distributed in the Sn phase. Sn grain size in the as-received solder decreased as a function of Zn content. No Cu–Zn IMC compound was found in all the as received Zn added solder. It was obvious that the solder matrix of as-received solder has changed after reflow. In general, Cu₆Sn₅ particles are larger after reflow by comparing Fig. 1e–h and Fig. 1a–d. After reflow, SAC + 0.3Zn and SAC + 0.5Zn have more rounded shaped Cu₆Sn₅ IMCs distributed in Sn phase in contrast with the elongated shaped Cu₆Sn₅ that was found SAC105 and SAC 105 + 0.1Zn.

3.2 Interfacial reaction after reflow and aging

Figure 2 shows the solder/Cu interface (cross-sectioned) after reflow and up to 1-month aging. After reflow, Cu₆Sn₅ layer with scallop morphology was forms at the solder/substrate interface (Fig. 2a). With addition of zinc, scallop type IMC are still seen, but their numbers are higher (Fig. 2b–d). Though the number of IMC scallop does not seem to change with the Zn content ranged from 0.1 to 0.5 wt%. A darker submicrometer thick Cu₃Sn layer in between the Cu₆Sn₅ layer and the Cu substrate was seen under very high magnification in all samples.

Solder joints were thermally aged at 150 °C (168 h and 720 h) to study the effects of Zn on the solid state reaction.

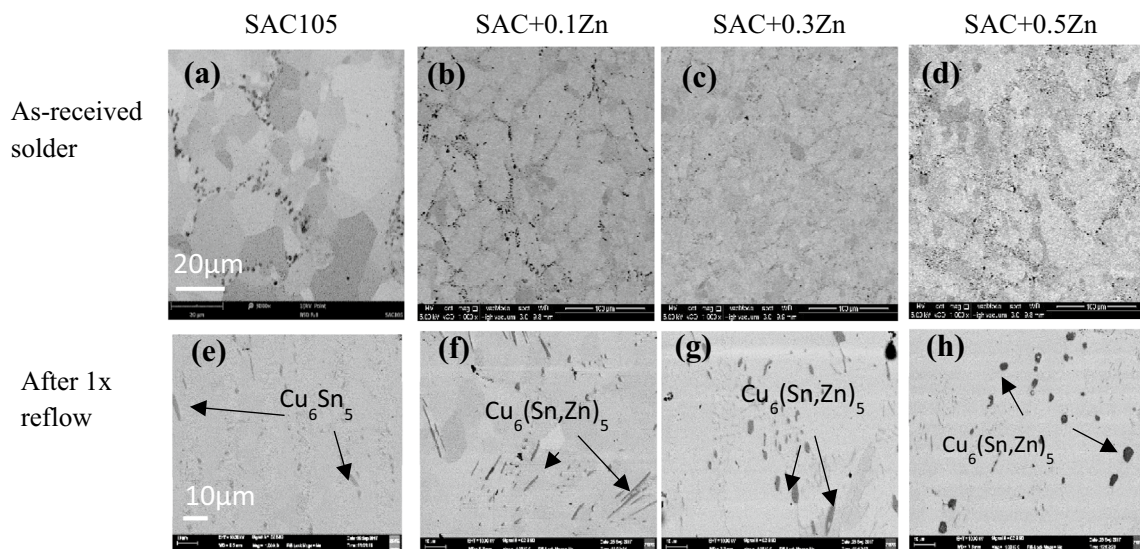


Fig. 1 Micrographs of cross sectioned solder matrix of as cast and after reflow of SAC105, SAC + 0.1Zn, SAC + 0.3Zn and SAC + 0.5Zn

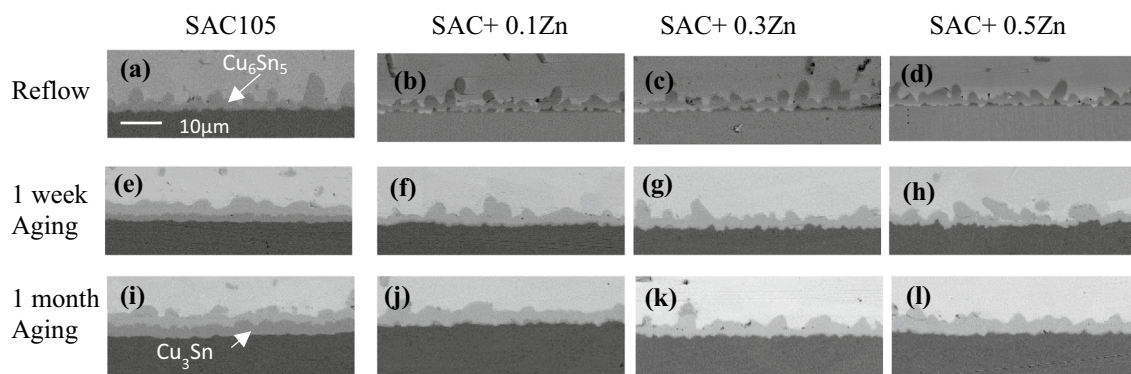


Fig. 2 Micrographs (cross sectioned) of the solder/copper interface after reflow (a–d), after 1 week aging (e–h) and after 1-month aging (i–l) of SAC105, SAC + 0.1Zn, SAC + 0.3Zn and SAC + 0.5Zn

The effect of Zn addition on the interfacial IMC thickness is more prominent after solid state annealing. Figure 2e–l shows the cross-sectional images of SAC105, SAC + 0.1Zn, SAC + 0.3Zn and SAC + 0.5Zn after 168 h and 720 h aging. After thermal aging for 168 h and 720 h, Cu_3Sn intermetallic layer (darker in contrast) Cu_3Sn formed in between the Cu_6Sn_5 and Cu substrate in SAC solder (Fig. 2e, 2i), while for sample with addition of Zn, submicron Cu_3Sn is discontinuous at the interface and could only be seen under high magnification. Trace of Zn is found in Cu_6Sn_5 and no Cu–Zn compound was found the interface of all SAC + Zn solders.

Figure 3 shows the graphs of IMC thickness versus Zn content. Effect of Zn addition on the interfacial IMC thickness is apparent after reflow, where the height of Cu_6Sn_5 is reduced with the addition of Zn. However, the thickness of the interfacial IMC does not seem to vary much as Zn

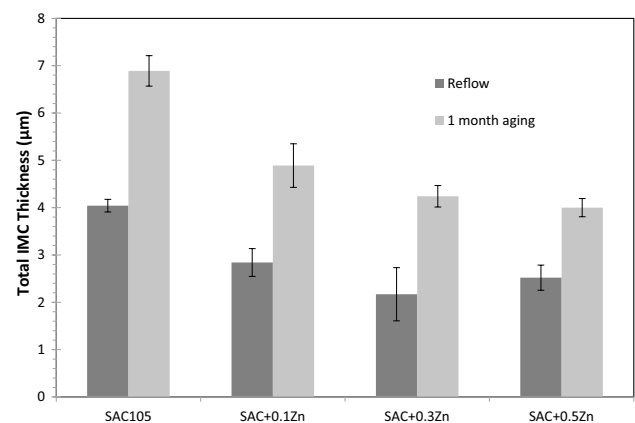


Fig. 3 Total thickness of interfacial IMC of SAC 105, SAC–0.1Zn, SAC + 0.3Zn and SAC + 0.5 Zn after reflow and after aging for 720 h

content increased from 0.1 to 0.5%. After thermal aging for 1 month, the total IMC is reduced as a function of Zn addition.

3.3 Zn distribution in $\text{Cu}_6(\text{Sn,Zn})_5$

Figure 4 shows the Zn elemental distribution in $\text{Cu}_6(\text{Sn,Zn})_5$ using EPMA. From Fig. 4, it is seen that the Zn concentration in $\text{Cu}_6(\text{Sn,Zn})_5$ increases with the increase of Zn% in SAC 105. For SAC 105 + 0.1Zn and SAC105 + 0.3Zn, the Zn distribution in $\text{Cu}_6(\text{Sn,Zn})_5$ was rather uniform after reflow. However, after aging up to 168 and 720 h, Zn tends to concentrate at the solder/ Cu_6Sn_5 interface and $\text{Cu}_6\text{Sn}_5/\text{Cu}$ interface. It was obvious that the concentration of Zn at the centre of Cu_6Sn_5 is low in SAC + 0.1Zn and SAC + 0.3Zn after aging (Fig. 4d, e, g, h). From Fig. 4c, f, i, it can be seen that the Zn concentration in $\text{Cu}_6(\text{Sn,Zn})_5$ is high in SAC105 + 0.5Zn compared with other samples. As the aging time increase, more Zn was seen distributed at the IMC/Cu interface. Figure 5 shows the Zn at.% in $\text{Cu}_6(\text{Zn, Sn})_5$ in SAC + 0.1Zn, SAC + 0.3Zn and SAC + 0.5Zn investigated by EPMA after aging up to 720 h. In general, the Zn at.% in $\text{Cu}_6(\text{Sn,Zn})_5$ increases with increase of Zn addition in SAC. After aging up to 720 h, it can be seen that the Zn at.% in $\text{Cu}_6(\text{Sn,Zn})_5$ in SAC 105 + 0.1 decreases as a function of aging time, while the Zn at.% in $\text{Cu}_6(\text{Sn,Zn})_5$ in SAC105 + 0.3Zn and SAC + 0.5Zn remain the same even after aging.

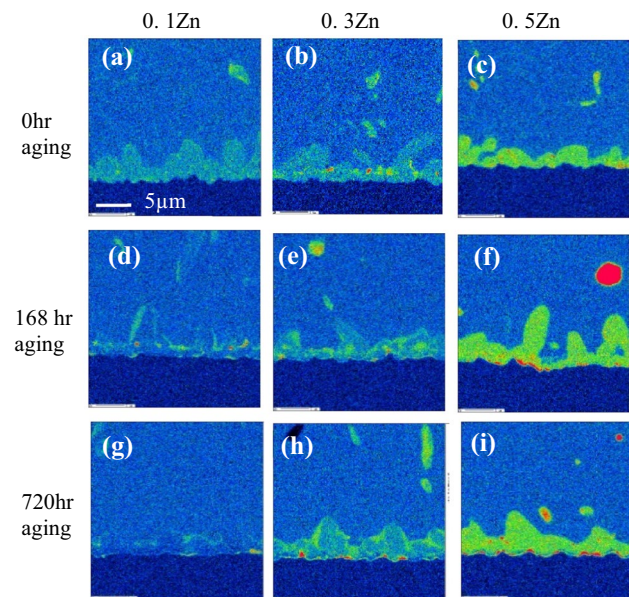


Fig. 4 Zn distribution maps at the solder/Cu interface in SAC+0.1Zn, SAC+0.3Zn and SAC+0.5Zn after aging 0 h, 168 h and 720 h

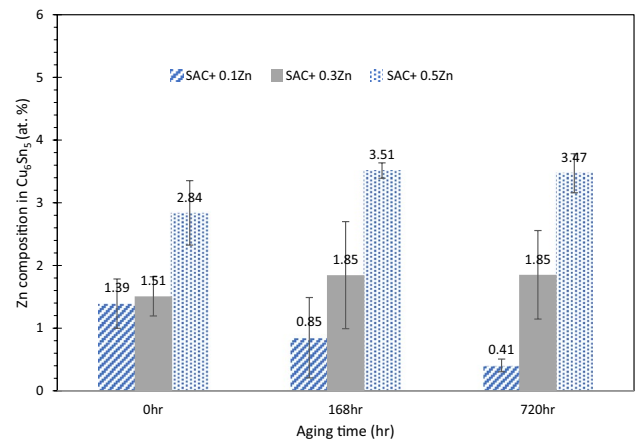


Fig. 5 Variation of Zn composition in $\text{Cu}_6(\text{Zn, Sn})_5$ in SAC+0.1Zn, SAC+0.3Zn and SAC+0.5Zn after aging at 0 h, 168 h and 720 h

3.4 IMC grain size at the Cu/solder interface

Figure 6 shows the top-view FESEM image of the interfacial IMC of SAC, SAC + 0.1Zn, SAC + 0.3Zn and SAC + 0.5Zn after reflow. All of the IMC grains seen on the etched surface of different samples were identified as Cu_6Sn_5 by EDX analysis. It could be seen that addition of Zn significantly reduced Cu_6Sn_5 grain size at the interface. Although the scallop morphology of the Cu_6Sn_5 did not change much in all samples, it could be seen that the Cu_6Sn_5 in SAC + Zn solders were slightly more faceted as compared to SAC105. As seen in Fig. 7, the number of Cu_6Sn_5 in a $10,000 \mu\text{m}^2$ area at the interface in SAC + Zn solder is almost 3–4 times more than that of SAC solder.

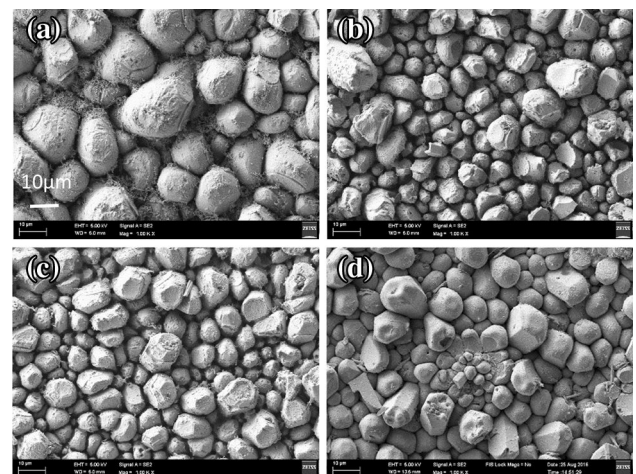


Fig. 6 FESEM top view image of IMC **a** SAC105, **b** SAC+0.1Zn, **c** SAC+0.3 Zn and **d** SAC+0.5Zn after reflow

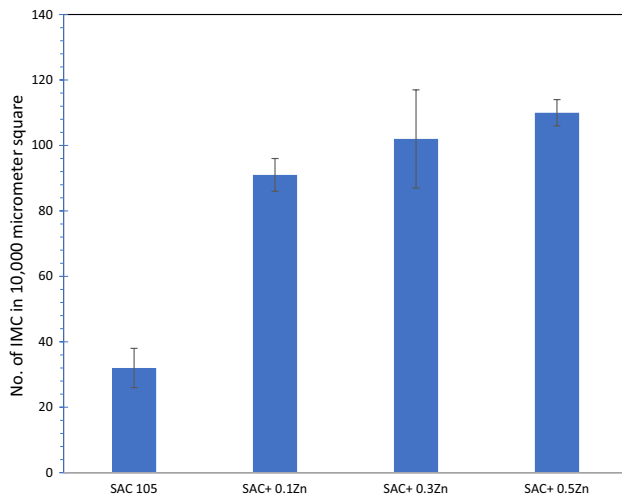


Fig. 7 Number of top Cu₆Sn₅ grains in 10,000 μm² in SAC105, SAC + 0.1Zn, SAC + 0.3Zn and SAC + 0.5Zn after reflow

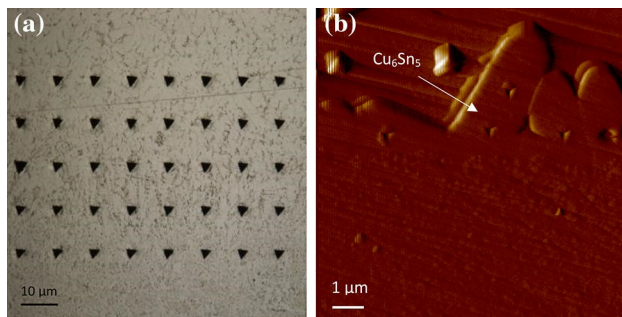


Fig. 8 **a** Optical micrograph of the indentation arrays on the eutectic region of bulk solder; **b** scanning probe microscopy image of Cu₆Sn₅ at the solder/Cu interface after indentation

3.5 Nanoindentation on Bulk solder

Figure 8 shows the array indentation in the bulk solder and the indentation on Cu₆Sn₅ at the solder/Cu interface. Bulk solder sample was tested after reflow, while Cu₆Sn₅ was tested after reflow and after aging for 720 h. Table 1

shows the average hardness and Young's Modulus in the bulk region and in Cu₆Sn₅ at the solder/Cu interface. For as-reflow sample, the hardness of the eutectic region and Cu₆Sn₅ increase as a function of Zn content. With the addition of Zn up to 0.5%, an increase of approximately ~25% is seen in H_{eutectic}, while H_{Cu₆Sn₅} increases from ~6.60 to 7.09 GPa. The addition of Zn does not appear to have significant effect on E_{eutectic}. After aging up to 720 h, Cu₆Sn₅ layer of all samples shows a decrease in hardness as compared to the as reflow sample. However, the hardness still shows an increasing trend as a function of Zn content.

The bulk solder of SAC, SAC + 0.1Zn and SAC + 0.5Zn were subjected to nanoindentation creep. Figure 9 shows the time-displacement curves for the samples. It is seen that the displacement increases abruptly as the load is applied at loading rate of 1 mN/s until it reaches the maximum load of 10 mN. This displacement is termed instantaneous displacement. As the load reached the peak, it was hold there for 900 s. During this hold period, the displacement continues to increase with time as the load is kept constant. This displacement is termed time-dependent displacement. Table 2 shows the measured instantaneous, time dependent, and total displacement of the samples. It is observed that addition of Zn in the solder does not have any significant effects on the instantaneous displacement. As for the time-dependent displacement, it decreases as a function of Zn, where SAC exhibits the highest time-dependent displacement ~6.1 μm, and SAC + 0.5 Zn shows the lowest displacement of ~4.5 μm. Thus, the total displacement has been reduced when Zn is added.

4 Discussion

From Fig. 1, the addition of Zn as minor alloying element has refined the bulk microstructure of SAC solder significantly. SAC solder has been reported to have large undercooling ranged ~17–30 °C [2]. These large undercoolings due to the delayed nucleation of β-Sn during solidification can permit extended formation of primary intermetallic compounds (IMCs) far from thermodynamic equilibrium.

Table 1 Hardness and modulus of bulk solder and Cu₆Sn₅ IMC in SAC105, SAC + 0.1Zn, SAC + 0.3Zn and SAC + 0.5Zn after 1 × reflow

Sample	Bulk solder		Cu ₆ Sn ₅			
	As reflow		As reflow		1 month aging	
	Hardness (GPa)	Young's Modulus (GPa)	Hardness (GPa)	Young's Modulus (GPa)	Hardness (GPa)	Young's Modulus (GPa)
SAC 105	0.148 ± 0.012	79.94 ± 6.49	6.60 ± 0.45	107.11 ± 8.50	6.28 ± 0.18	103.15 ± 8.50
SAC + 0.1Zn	0.153 ± 0.012	82.74 ± 6.61	6.78 ± 0.8	103.48 ± 10.08	6.21 ± 0.23	105.28 ± 10.09
SAC + 0.3Zn	0.164 ± 0.021	76.42 ± 8.06	6.93 ± 0.3	120.36 ± 6.61	6.55 ± 0.33	102.76 ± 7.62
SAC + 0.5Zn	0.184 ± 0.016	76.42 ± 5.56	7.09 ± 0.37	117.63 ± 8.43	6.65 ± 0.38	119.01 ± 13.27

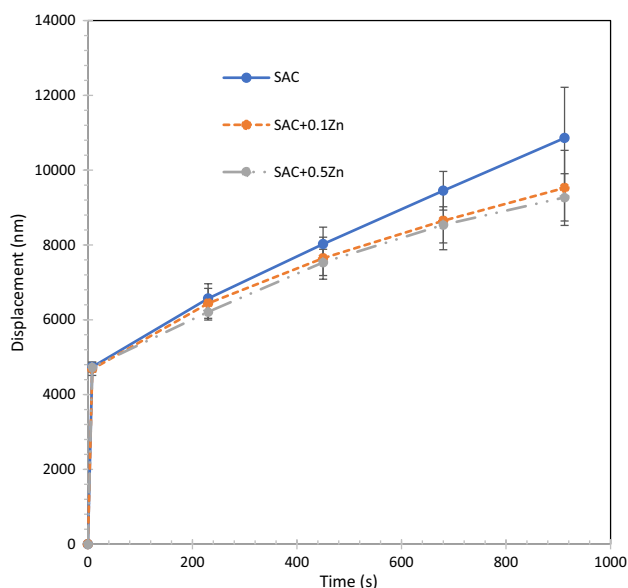


Fig. 9 Average time–displacement curves for SAC, SAC+0.1Zn and SAC+0.5Zn

This results in large β -Sn dendrites, large grains, reduced amounts of eutectic, and undesired morphologies of the intermetallic compounds (e.g., large Ag_3Sn plates or long Cu_6Sn_5 needles) [2, 32]. Hence, large undercooling of β -Sn was responsible for the coarsening of SAC microstructure which reduced the reliability of solder joints. It has been reported that adding minor alloying element into solder could reduced the undercooling of solder. Addition of minor alloying element reduced undercooling by promoting nucleation of β -Sn. Minor alloying atoms can exist as solutes or compounds (formed by reacting with element in solders e.g. Sn, Cu, Ag) in molten Sn where it acts as a heterogeneous site for β -Sn to nucleate [33]. Many studies reported that the addition of Zn can reduce undercooling of SAC significantly, where it could lower the undercooling ranging from 1–8 °C [2, 13, 16, 34]. Many studies on the effect of Zn on the melting characteristic of SAC has suggested that even with a minimal Zn addition (as low as 0.1 wt%) could reduce the undercooling of β -Sn significantly [35]. It is believed that Zn which is easily oxidised formed small solid zinc oxide, ZnO particles within molten solder during heating, this act as heterogeneous nucleants for β -Sn which results in minimizing undercooling and provide more refined microstructures [36].

Figure 3 shows that Zn addition has decreased the growth of Cu_6Sn_5 and suppressed the formation of Cu_3Sn during thermal aging. Many studies have been done on the effect of Zn on the Cu–Sn reaction, where Zn as alloying element was found to be effective in suppressing the growth of interfacial Cu_6Sn_5 and Cu_3Sn layers. As mentioned earlier in the introduction, minor alloying elements that have influence on Cu–Sn IMC growth have been divided into two categories. Zn obviously fall under category 1 (element that is soluble in Cu–Sn IMC) as can be seen from Figs. 5, 6, 7) where it shows marked solubility in Cu_6Sn_5 . Although the solubility of Zn in Cu_3Sn was not able to be quantified in this study due to the submicron size of the Cu_3Sn layer which is due to suppression of Zn, it has been reported that Zn is soluble in both Cu_6Sn_5 and Cu_3Sn and that Zn goes to Sn sublattice in both compounds [$\text{Cu}_6(\text{Sn},\text{Zn})_5$ and $\text{Cu}_3(\text{Sn},\text{Zn})$]. Reported solubility values are (at 250 °C) 6 at.% of Zn to Cu_6Sn_5 and 9 at.% to Cu_3Sn , respectively [17]. A few studies have tried to explain the mechanism through which Zn alloying affects the growth of interfacial IMC between the solder and Cu substrate. So far there are two main approaches or theories on how Zn could suppress the growth of IMC. During aging, Cu_6Sn_5 IMC layer grows by interdiffusion of Cu and Sn, and the reaction with between Cu and Sn. On the other hand, it was suggested that Cu_3Sn IMC grows by reaction between the Cu substrate and Cu_6Sn_5 IMC, following the equation [10]:



For this approach, Kang et al. suggested that Zn atoms have a tendency to accumulate at the $\text{Cu}_6\text{Sn}_5/\text{Cu}$ interface. Under high resolution STEM, Kang et al. noticed Zn atoms exist in a Cu–Zn solid solution between IMC and Cu substrate [14]. By their presence at the interface, Zn atoms hinder the flow of copper atom to react with Cu_6Sn_5 and thereby retarding IMC growth [12]. The second approach is through thermodynamic explanation. This approach is used to explain the suppression of Cu_3Sn when Ni, Co, Pt and Au are used as minor alloying element. These elements stabilize Cu_6Sn_5 and hinder the growth of Cu_3Sn . Thus, in this study, it is suggested that Zn dissolves into Cu_6Sn_5 to form $\text{Cu}_6(\text{Sn},\text{Zn})_5$ during reflow and then stabilizes it against the growth of Cu_3Sn during thermal aging [10]. However, different from the addition of Ni, Co, Pt and Au, Zn was found to reduce the growth of Cu_6Sn_5 as well during thermal aging,

Table 2 Instantaneous, total, time-dependent displacement of bulk solder in SAC 105, SAC+0.1Zn and SAC+0.5Zn

Sample	Instantaneous displacement(μm)	Time dependent displacement (μm)	Total displacement (μm)
SAC 105	4.74 ± 0.14	6.12 ± 0.45	10.86 ± 0.59
SAC+0.1Zn	4.68 ± 0.19	4.85 ± 0.79	9.53 ± 0.97
SAC+0.5Zn	4.73 ± 0.12	4.53 ± 0.62	9.26 ± 0.73

while addition of Ni, Co, Pt and Au has increased the growth of Cu_6Sn_5 due to the more stabilized $\eta\text{-Cu}_6\text{Sn}_5$ phase [10].

One possible reason for why stabilization of $\text{Cu}_6(\text{Sn},\text{Zn})_5$ does not increase the growth of Cu_6Sn_5 but suppress Cu_3Sn during aging could be explained by the synergy effect from both theories suggested above. During reflow, Zn dissolves into Cu_6Sn_5 to form a stabilize $\text{Cu}_6(\text{Sn},\text{Zn})_5$, and Zn tends to accumulate at the edge of solder/IMC and especially at the IMC/Cu interface (Fig. 5). Accumulation of Zn atoms as Cu–Zn solid solution formed at the IMC/Cu interface because the value of ΔG_f (Gibbs energy of formation) and the activation energy of growth of Cu–Zn IMC was more negative than that of Cu–Sn IMC at 230–280 °C [37–39]. Besides that, accumulation of Zn at the edge of solder/IMC could be due to the segregation at the interphase boundary phenomenon where Zn solute segregated at the interphase grain boundary as there are lower energy sites at the grain boundary than in the bulk [40, 41]. During isothermal aging, with stabilized $\text{Cu}_6(\text{Sn},\text{Zn})_5$ against the growth of Cu_3Sn and along with the flow of Cu atom hindered by the presence of Zn at IMC/Cu interface, it seems impossible for the growth of Cu_3Sn . Besides, the presence of Zn at solder/IMC could have hindered Sn atom for the formation of Cu_6Sn_5 . Presence of Zn at both interface has slow down the interdiffusion of Cu atom and Sn atom, thus unlike addition of Ni, Co, Pt and Au, the thickness of Cu_6Sn_5 does not increased in SAC105 + Zn solder.

For the reflowed SAC + Zn solder joints, distribution of Zn atom was relatively homogenous in $\text{Cu}_6(\text{Sn},\text{Zn})_5$. However, after subsequent annealing for 168 h and 720 h, it is observed that Zn tends to segregate at the Sn/IMC and IMC/Cu interface in SAC + 0.1Zn and SAC + 0.3Zn, leaving the centre of the IMC scarce with Zn distribution. It should be noted that only Zn was found segregated in $\text{Cu}_6(\text{Sn},\text{Zn})_5$ while we do not see segregation/compositional gradient of other elements such as Sn, Cu, Ag in $\text{Cu}_6(\text{Sn},\text{Zn})_5$ interface. Segregation of Zn has also been observed at the IMC/solder interface in Sn–Bi alloys recently [42]. Ni was also found to segregate at the interface after reflow as well as after aging [43, 44].

From Fig. 8, SAC + Zn solder has increased the number of Cu_6Sn_5 grain at the Cu/solder significantly. Experimental and theoretical work show that the nucleation rate and growth of IMC grains can be controlled by the IMC/liquid interface energy [45–47]. From thermodynamic considerations, higher $\gamma_{\text{Solder}/\text{Cu}_6\text{Sn}_5}$ would promote the formation of semi-spherical IMC grains while the low $\gamma_{\text{Solder}/\text{Cu}_6\text{Sn}_5}$ would promote the growth of an irregular or facet morphology in the IMC compound grains. Kotadia et al. suggested the influence of Zn on the Cu_6Sn_5 can be caused by absorption of Zn atoms from the bulk solder into the Cu_6Sn_5 forming the stable $\text{Cu}_6(\text{Sn},\text{Zn})_5$ and thus changes the interfacial energy between the molten solder and IMC grains, $\gamma_{\text{Solder}/\text{Cu}_6\text{Sn}_5}$

[13]. Phase-field modelling studies show that presence of Zn at the Cu_6Sn_5 would lower the interface liquid/ Cu_6Sn_5 interface energy and thus induces a more rapid nucleation of Cu_6Sn_5 grains [13].

Presence of Zn in SAC solder has increase the nano-hardness of the solder joint. Besides, addition of Zn has improved the creep behaviour of SAC as well, where it has lowered the time dependent displacement. Instantaneous displacement is related to plasticity whereas time dependent displacement is related to creep phenomenon [48]. For deformation at low temperature, low-temperature plasticity by dislocation glide is determined by (a) limited by a lattice resistance, (b) limited by discrete obstacles, (c) limited by phonon or other drags and (d) influenced by adiabatic heating [49]. Solid solution effect was not expected to play a role in the bulk microstructure as the solubility of Zn in Sn negligible [50]. The increase of hardness and improving of creep in the bulk solder with addition of Zn is believed mainly due to the microstructural refinement of the eutectic region and IMC. Hardness of Cu_6Sn_5 increase as a function of Zn solubility in Cu_6Sn_5 . It is suggested that the incorporation of Zn in the IMC lattice has increased the lattice resistance. This is in good agreement with studies done by Chen et al. where they have calculated that the binding energy in the $\eta\text{-Cu}_6\text{Zn}_{0.5}\text{Sn}_{4.5}$ to be stronger than that of $\eta\text{-Cu}_6\text{Sn}_5$ [19]. That is to say, $\text{Cu}_6(\text{Sn},\text{Zn})_5$ is more resistant to deformation than Cu_6Sn_5 , which is considered to be the dominant factor in improving the hardness Cu_6Sn_5 .

Although only minimal Zn was added into SAC105, Zn is clearly seen to have significant influences on the nanohardness, creep, and the interfacial characteristics during reflow and thermal aging. However, the amount of Zn must be kept below 0.6 wt% in order to formation of brittle Cu_5Zn_8 , also for the reason of its poor oxidation and poor corrosion resistance in humid high-temperature environment.

5 Conclusion

Based on this study, the following conclusions are drawn:

- Zn atoms tends to segregate at the Sn/ Cu_6Sn_5 and $\text{Cu}_6\text{Sn}_5/\text{Cu}_3\text{Sn}$ interface after reflow.
- Minor addition of Zn has increased the Cu_6Sn_5 grains at the interface significantly. It is suggested that accumulation of Zn at the Cu interface act as a preferential site to promote heterogeneous nucleation of Cu_6Sn_5 .
- Addition of Zn has reduced the thickness of Cu_6Sn_5 and hinder the formation of Cu_3Sn layer at the interface significantly during isothermal aging.
- It is suggested that Zn impart its influence on the interfacial reaction by stabilizing $\text{Cu}_6(\text{Sn},\text{Zn})_5$ and hindering

the flow of reacting species at the interface during reflow and thermal aging.

- Addition of Zn as minor alloying element has increased the hardness and creep behaviour of bulk microstructure. Besides that, hardness of $\text{Cu}_6(\text{Sn,Zn})_5$ is increased as a function of Zn composition in $\text{Cu}_6(\text{Sn,Zn})_5$.

Acknowledgments The authors would like to acknowledge the financial support from Postgraduate Research Grant (PPP), University of Malaya (Project No. PG176-2016A).

References

1. Official Journal of the European Union, DIRECTIVE 2002/95/EC OF The European Parliament and of the Council (2003)
2. S.K. Kang, D.Y. Shih, D. Leonard, N.Y. Donald, D.W. Henderson, T. Gosselin, A. Sarkhel, N.Y.C. Goldsmith, *JOM* **56**, 34 (2004)
3. C. Handwerker, U. Kattner, K.-W. Moon, *Fundamental Properties of Pb-Free Solder Alloys* (Springer, New York, 2007)
4. W. Liu, N.C. Lee, *JOM* **56**, 26 (2007)
5. T. Lee, T.R. Bieler, C. Kim, H. Ma, *Fundamentals of Lead-Free Solder Interconnect Technology* (Springer, New York, 2015)
6. A.E. Ahmad, *Mater. Des.* **52**, 663 (2013)
7. K.S. Kim, S.H. Huh, K. Suganuma, *Microelectron. Reliab.* **43**, 259 (2003)
8. I.E. Anderson, J.W. Walleiser, H.F. Laabs, A. Kracher, *J. Electron. Mater.* **38**, 2770 (2010)
9. Y.W. Shi, J. Tian, H. Hao, Z. Xia, L.F. Guo, *J. Alloys Compd.* **453**, 180 (2008)
10. T. Laurila, V. Vuorinen, M. Paulasto-Kröckel, *Mat. Sci. Eng. R.* **68**, 1 (2010)
11. S. Lei, L. Zhang, *Adv. Mater. Sci. Eng.* **2**, 16 (2015)
12. S.K. Kang, D.Y. Shih, D. Leonard, L. Gignac, D.W. Henderson, S. Cho, *J. Electron. Mater.* **35**, 479–485 (2007)
13. H.R. Kotadia, O. Mokhtari, O.M. Bottrill, M.P. Clode, M.A. Green, S.H. Mannan, *J. Electron. Mater.* **39**, 2720 (2010)
14. M. Cho, S. Kang, S.Y. Shih, D.Y. J. *Electron. Mater.* **36**, 1501 (2007)
15. M. Amagai, *Microelectron. Reliab.* **48**, 1–16 (2008)
16. I.E. Anderson, J.W. Walleiser, J.L. Harringa, *J. Electron. Mater.* **38**, 2770 (2009)
17. C.Y. Chou, S.W. Chen, *Acta Mater.* **54**, 2393 (2006)
18. C.C. Yu, J.-G. Duh, *Scr. Mater.* **65**, 783 (2011)
19. S. Chen, W. Zhou, P. Wu, *J. Electron. Mater.* **44**, 3920 (2015)
20. A.S. Maxwell, M.A. Monclus, N.M. Jennet, G. Dean, *Polym. Test* **30**, 366–371 (2011)
21. W.M. Roellig, M. Mueller, K.-J. Wolter, *Microelectron. Reliab.* **48**, 843 (2008)
22. V.M.F. Marques, C. Johnston, P.S. Grant, *Act. Mater.* **61**, 2460 (2013)
23. V.M.F. Marques, B. Wunderle, C. Johnston, P.S. Grant, *Acta Mater.* **61**, 2471 (2013)
24. D. Mu, H. Huang, K. Nogita, *Mater. Lett.* **86**, 46 (2012)
25. D. Mu, H. Huang, S.D. Macdonald, K. Nogita, *J. Electron. Mater.* **42**, 304 (2012)
26. D. Mu, H. Huang, S.D. McDonald, J. Read, K. Nogita, *Mater. Sci. Eng. A* **566**, 126 (2013)
27. P.Y. Chia, A.S.M.A. Haseeb, S.H. Mannan, *Materials* **9**, 430 (2016)
28. F. Gao, T. Takemoto, H. Nishikawa, *J. Electron. Mater.* **35**, 905 (2006)
29. Y.M. Leong, A.S.M.A. Haseeb, *Materials* **9**, 522 (2016)
30. W.C. Oliver, G.M.J. Pharr, *Mater. Res.* **19**, 3 (2004)
31. M.A. Meyers, K. Chawla, *Mechanical Behavior of materials* (Cambridge University Press, Cambridge, 2008)
32. A. LaLonde, D. Emelander, J. Jeannette, C. Larson, W. Rietz, D. Swenson, D.W. Henderson, *J. Electron. Mater.* **33**, 1545 (2004)
33. H. Shang, Z.L. Ma, S.A. Belyakov, C.M. Gourlay, *J. Alloys Compd.* **715**, 471 (2017)
34. J. Mao, B. Reeves, B. Lenz, D. Ruscitto, D. Lewis, *J. Electron. Mater.* **46**, 6319 (2017)
35. K. Subramaniam, *Lead-Free Solders: Materials Reliability for Electronics* (Wiley, New York, 2012)
36. D. Swenson, *J. Mater. Sci.: Mater. Electron.* **18**, 39 (2007)
37. T. Gancarz, *Mater. Lett.* **171**, 187–190 (2016)
38. J.M. Song, *J. Mater. Res.* **22**, 4332–4433 (2007)
39. C.S. Lee, F.S. Shieu, *J. Electron. Mater.* **35**, 1660–1664 (2006)
40. G. Bruggeman, E.B. Kula, *Segregation at Interphase Boundaries. Surfaces and Interfaces II* (Springer, Boston, 1968)
41. S.-J.L. Sintering, *Sintering* (Elsevier, Amsterdam, 2005)
42. S. Zhou, O. Mokhtari, M.G. Rafique, V.C. Shunmugasamy, B. Mansoor, H. Nishikawa, *J. Alloys Compd.* **765**, 1243 (2018)
43. S.L. Tay, A.S.M.A. Haseeb, M.R. Johan, P.R. Munroe, M.Z. Qadir, *Intermetallics* **33**, 8 (2013)
44. G. Zeng, D. Stuart, D. McDonald, D. Mu, Y. Terada, H. Yasuda, O. Gu, K. Nogita, *Intermetallics* **54**, 20–27 (2014)
45. M.S. Park, R. Arroyave, *Acta Mater.* **60**, 923 (2012)
46. H. Zhang, X.Y. Wang, L.L. Zheng, S. Sampath, *Int. J. Heat Mass Transfer.* **47**, 2191 (2004)
47. M.S. Park, R. Arróyave, *Acta Mater.* **58**, 4900 (2010)
48. A.C. Fischer-Cripps, *Mater. Sci. Eng., A* **385**, 74 (2004)
49. H.J. Frost, M.F. Ashby, *Deformation Mechanism Maps* (Pergamon Press, Oxford, 1982)
50. H. Ohtani, M. Miyashita, K. Ishida, *J. Jpn Inst. Metals* **63**, 685 (1999)

Publisher's Note Springer Nature remains neutral with regard to jurisdictional claims in published maps and institutional affiliations.